POLITECNICO DI TORINO
Repository ISTITUZIONALE

THz electrodynamics of BaFe1.91Ni0.09As2 film analyzed in the framework of multiband Eliashberg
theory

(Article begins on next page)

29 March 2024

THz electrodynamics of BaFe1.91Ni0.09As2 film analyzed in the framework of multiband Eliashberg theory

THz electrodynamics of $BaFe_{1.91}Ni_{0.09}As_2$ film analyzed in the framework of multiband Eliashberg theory

G.A. Ummarino[1,2]**, A.V. Muratov**[3]**, L.S. Kadyrov**[4]**, B.P. Gorshunov**[4]**, S. Richter**[5,6]**, A. Anna Thomas**[5,6]**, R. Hühne**[5] **and Yu.A. Aleshchenko**[3]

E-mail: `aleshchenkoya@lebedev.ru`

[1] Istituto di Ingegneria e Fisica dei Materiali, Dipartimento di Scienza Applicata e Tecnologia, Politecnico di Torino, Corso Duca degli Abruzzi 24, 10129 Torino, Italy
[2] National Research Nuclear University MEPhI (Moscow Engineering Physics Institute), Kashirskoe shosse 31, Moscow 115409, Russia
[3] P.N. Lebedev Physical Institute, Russian Academy of Sciences, Leninskiy Prospekt 53, Moscow 119991, Russia
[4] Moscow Institute of Physics and Technology, Institutskiy per. 9, Dolgoprudny, Moscow Region, 141700, Russia
[5] Institute for Metallic Materials, Leibniz IFW Dresden, Helmholtzstrasse 20, Dresden 01069, Germany
[6] School of Sciences, TU Dresden, 01062 Dresden, Germany

Abstract.   The temperature dependences of the plasma frequency, superfluid density and London penetration depth were determined from terahertz spectra of conductivity and dielectric permittivity of $BaFe_{1.91}Ni_{0.09}As_2$ film with critical temperature $T_c = 19.6$ K. Part of experimental data were analyzed within a simple three-band Eliashberg model where the mechanism of superconducting coupling is mediated by antiferromagnetic spin fluctuations, whose characteristic energy Ω_0 scales with T_c according to the empirical law $\Omega_0 = 4.65k_BT_c$, and with a total electron-boson coupling strength $\lambda_{tot} = 2.17$.

PACS numbers: 74.70.Xa, 74.20.Fg, 74.25.Kc, 74.20.Mn

THz electrodynamics of $BaFe_{1.91}Ni_{0.09}As_2$ film analyzed in the framework of multiband Eliashberg theory 2

1. Introduction

Iron based superconductors are nowadays among the most studied superconducting (SC) materials due to their potential technological impact and their intriguing fundamental multiband and pairing properties. The widely accepted pairing state of most iron based superconductors and, in particular, of the compounds based on doped $BaFe_2As_2$ (Ba122-family) is the fully gapped $s_\pm$ phase [1, 2]. However, a possibility of the broken time-reversal symmetry in the SC state has been shown recently [3] for instance in $(Ba,K)Fe_2As_2$ at high doping levels by means of muon spin-relaxation measurements. This indicates the presence of the chiral type order parameter of either $s + is$ or $s + id$ symmetry. Typically the Fermi surface in these materials at the optimal doping level consists of holelike pockets at the Γ point and electronlike pockets centered at the $X(0, \pm\pi)$ points of the Brillouin zone. The pairing state consists of an extended s-wave pairing with a sign reversal of the order parameter between different Fermi surface sheets and with interband coupling between hole and electron bands provided by antiferromagnetic spin fluctuations. Although this model is widely accepted, direct experimental confirmations are rare [4].

Many doped SC compounds of the Ba122-family, especially Co- and K-doped, can be grown as epitaxial thin films with decent quality. However optical studies of Ni-doped Ba122 epitaxial films have been reported only in [5]. Moreover, even for a bulk $Ba(Fe,Ni)_2As_2$ data on the SC gap are scarce [6, 7, 8, 9, 10].

In this paper, we apply the Eliashberg model to describe SC properties of the $BaFe_{1.91}Ni_{0.09}As_2$ film probed by the terahertz (THz) spectroscopy. Measurements in the THz region has proven to be of particular importance in detecting the presence of SC gaps in superconductors, including multiband systems [11].

2. Experiment

The nearly optimum electron doped $BaFe_{1.91}Ni_{0.09}As_2$ film with a thickness of 120 ± 10 nm was grown by pulsed laser deposition (PLD) on polished (001) CaF_2 substrate. More details on the sample preparation are in [12, 13, 14]. The results of measurement of the SC transition temperature T_c of Ni-Ba122 film by an inductive technique [15] are shown in Fig. 1. A sharp SC transition was found at $T_c = 19.6$ K.

THz spectroscopic measurements of the Ni-Ba122 film on the CaF_2 substrate were carried out in the transmission mode with the Menlo pulsed time-domain THz spectrometer within the range of 10–50 cm^{-1} (wavelengths 1 mm–200 μm) at different temperatures down to $T = 5$ K with a home-made optical cryostat. The measured transmission coefficient and the phase shift of the electromagnetic radiation allow us to determine directly the spectra of real and imaginary parts of the complex dielectric permittivity $\hat{\varepsilon}(\omega) = \varepsilon_1(\omega) + i\varepsilon_2(\omega)$ and the complex optical conductivity $\hat{\sigma}(\omega) = \sigma_1(\omega) + i\sigma_2(\omega)$ without using the Kramers-Kronig relation [16]. The dielectric properties of the CaF_2 substrate were measured beforehand.

*THz electrodynamics of $BaFe_{1.91}Ni_{0.09}As_2$ film analyzed in the framework of multiband Eliashberg theory*3

3. Results

In this work, we focus on the itinerant charge-carrier response contained within the THz spectral range. The spectra of dielectric permittivity and conductivity of $BaFe_{1.91}Ni_{0.09}As_2$ film both in normal (a,c) and SC states (b,d) are displayed in Fig. 2. The abrupt decrease in the low-frequency permittivity $\varepsilon_1(\omega, T)$ at $T \leqslant T_c$ shown in Fig. 2(b) evidences the inductive response of the SC condensate. This behavior is fitted with the expression $\varepsilon_1 \propto -(\omega_{p,s}/\omega)^2$ (solid line), where $\omega_{p,s}$ is the SC plasma frequency. This fit allows us to determine $\omega_{p,s}$. The solid lines in Fig. 2(a), (c) and (d) are only guides to eye. At high temperatures, the THz conductivity is nearly frequency independent (see Fig. 2(c)). At $T < T_c$, the THz conductivity decreases due to the opening of the SC gap Fig. 2(d). It is easily recognized that even at the lowest temperature (5 K), i.e. $0.25T_c$, the gapping is not complete. According to [17], the presence of a finite conductivity at low frequencies well into the SC state could be due to a gap anisotropy of the electron pocket [18, 19, 20, 21]; impurity localized levels inside an isotropic gap [22, 23, 24]; or pair breaking due to interband impurity scattering in an $s_\pm$ symmetric gap [25, 26].

Figure 3 shows the calculated temperature dependences of the SC plasma frequency $\omega_{p,s}$ and the London penetration depth λ_L (right scale) determined as $\lambda_L = c/\omega_{p,s}$ [27]. The temperature dependence of the superfluid density $n_s = [\lambda_L(0)/\lambda_L(T)]^2$ is shown in the inset. A rough estimate of $\lambda_L(0) = 0.414$ μm can be made assuming a parabolic dependence for $\lambda_L(T)$ and using three low-temperature points of this dependence (at higher temperatures this parameter is affected by the sample geometry and fluctuations). Such behavior is compatible with nodes in the SC gap [28] or a multigap system [25]. To describe these experimental findings, an Eliashberg theory for $Ba(Fe,Ni)_2As_2$ has been developed.

4. The Model

The electronic structure of the compound $BaFe_{1.91}Ni_{0.09}As_2$, being very similar to Co doped case, can be approximately described by a three-band model with one hole band (indicated in the following as band 1) and two electron bands (indicated in the following as bands 2 and 3) [29]. In this way the gap of the hole band, Δ_1, has opposite sign to the two gaps residing on the electron bands, Δ_2 and Δ_3. The interband coupling between hole and electron bands ($s_\pm$ wave model [30, 2]) is mainly provided by antiferromagnetic spin fluctuations (sf), while phonons can be responsible for the intraband coupling (ph) [2]. The antiferromagnetic spin fluctuation coupling between bands with the same type of charge carriers (holes with holes and electrons with electrons) is zero while the phonon coupling is negligible [30, 2]. We assume that the symmetry of this system is $s_\pm$ for experimental and theoretical reasons. The experimental reasons are that almost all iron pnictides are $s_\pm$ and $Ba(Fe,Ni)_2As_2$ is very similar to Co doped case that is thought to be $s_\pm$ [31]. From a theoretical point of view, we use the theory developed in [32]

where, within a Ginzburg-Landau formalism, the necessary and sufficient conditions to realize a $s_\pm$ state (π state) are established analytically. It is necessary to premise that in our model, as we will see, the electron-boson coupling is just from antiferromagnetic spin fluctuations because we neglect the phonons. We will find the coupling constants $\lambda_{12} = -0.91$ and $\lambda_{13} = -1.356$ (they are positive in the paper because we, as usually, change the sign inside the equations) and $\lambda_{23} = 0$. Of course λ_{23} differs from zero and is positive but small because is connected with the phonon contribution. We have verified in the past [33] that small phononic couplings (very small compared to the coupling value of antiferromagnetic spin fluctuations) do not change the result of the numerical simulations and, for simplicity and to reduce the number of free parameters, they have been set to zero. In [32] the functions G_1, G_2 and G_3 are defined as $G_1 = \frac{\lambda_{12}}{|\lambda_{23}|}\frac{|\psi_1|}{|\psi_2|}$, $G_2 = sign(\lambda_{23})$ and $G_3 = \frac{\lambda_{13}}{|\lambda_{23}|}\frac{|\psi_3|}{|\psi_2|}$. G_1 and G_3 are negative and large and G_2 is positive and small since $\lambda_{23} \approx 0$ and the ψ_i are more or less of the same order of magnitude because they are proportional to square root of superfluid densities n_i in the bands 1, 2 and 3 (that we have calculated for obtaining the penetration depth). We are in the low left corner of Fig. 2 of the same paper where the solution π is stable. To calculate the gaps and the critical temperature within the $s_\pm$ wave three-band Eliashberg equations [34, 35, 36], one has to solve 6 coupled equations for the gaps $\Delta_i(i\omega_n)$ and the renormalization functions $Z_i(i\omega_n)$, where i is a band index (that ranges between 1 and 3) and ω_n are the Matsubara frequencies. The imaginary-axis equations [33, 37, 38] read:

$$\omega_n Z_i(i\omega_n) = \omega_n + \pi T \sum_{m,j} \Lambda_{ij}^Z(i\omega_n, i\omega_m) N_j^Z(i\omega_m) +$$

$$+ \sum_j [\Gamma_{ij}^N + \Gamma_{ij}^M] N_j^Z(i\omega_n) \tag{1}$$

$$Z_i(i\omega_n)\Delta_i(i\omega_n) = \pi T \sum_{m,j} [\Lambda_{ij}^\Delta(i\omega_n, i\omega_m) - \mu_{ij}^*(\omega_c)] \times$$

$$\times \Theta(\omega_c - |\omega_m|) N_j^\Delta(i\omega_m) + \sum_j [\Gamma_{ij}^N - \Gamma_{ij}^M] N_j^\Delta(i\omega_n) \tag{2}$$

where Γ_{ij}^N and Γ_{ij}^M are the scattering rates from non-magnetic and magnetic impurities, $\Lambda_{ij}^Z(i\omega_n, i\omega_m) = \Lambda_{ij}^{ph}(i\omega_n, i\omega_m) + \Lambda_{ij}^{sf}(i\omega_n, i\omega_m)$ and $\Lambda_{ij}^\Delta(i\omega_n, i\omega_m) = \Lambda_{ij}^{ph}(i\omega_n, i\omega_m) - \Lambda_{ij}^{sf}(i\omega_n, i\omega_m)$ where

$$\Lambda_{ij}^{ph,sf}(i\omega_n, i\omega_m) = 2 \int_0^{+\infty} d\Omega \Omega \alpha_{ij}^2 F^{ph,sf}(\Omega)/[(\omega_n - \omega_m)^2 + \Omega^2].$$

Θ is the Heaviside function and ω_c is a cutoff energy. The quantities $\mu_{ij}^*(\omega_c)$ are the elements of the 3×3 Coulomb pseudopotential matrix. Finally, $N_j^\Delta(i\omega_m) = \Delta_j(i\omega_m)/\sqrt{\omega_m^2 + \Delta_j^2(i\omega_m)}$ and $N_j^Z(i\omega_m) = \omega_m/\sqrt{\omega_m^2 + \Delta_j^2(i\omega_m)}$. The electron-boson coupling constants are defined as $\lambda_{ij}^{ph,sf} = 2 \int_0^{+\infty} d\Omega \frac{\alpha_{ij}^2 F^{ph,sf}(\Omega)}{\Omega}$. The solution of equations 1 and 2 requires a huge number of input parameters (18 functions and 27 constants), i.e.: i) nine electron-phonon spectral functions $\alpha_{ij}^2 F^{ph}(\Omega)$; ii) nine electron-antiferromagnetic

spin fluctuation spectral functions, $\alpha_{ij}^2 F^{sf}(\Omega)$; iii) nine elements of the Coulomb pseudopotential matrix $\mu_{ij}^*(\omega_c)$; iv) nine nonmagnetic Γ_{ij}^N and nine paramagnetic $\Gamma_{ij}^M = 0$ impurity-scattering rates. However, some of these parameters can be extracted from experiments and some can be fixed by suitable approximations. In particular, we refer to experimental data taken on high quality films, so we can rather safely assume a negligible disorder: the scattering from non-magnetic impurities Γ_{ij}^N can thus be taken to be zero. The same can be done for the scattering rate from magnetic impurities: $\Gamma_{ij}^M = 0$. At least as a starting point, let us make further assumptions that have been shown to be valid for iron pnictides [33, 37, 38]. Following ref. [2], we can thus assume that: i) the total electron-phonon coupling constant is small (the upper limit of the phonon coupling in the usual iron-arsenide compounds is ≈ 0.35 [39]); ii) phonons mainly provide *intra*band coupling so that $\lambda_{ij}^{ph} \approx 0$; iii) spin fluctuations mainly provide *interband coupling between hole and electron bands*, so that $\lambda_{ii}^{sf} \approx 0$. Moreover, we put in first approximation the phonon contribution to *intra*band coupling equal to zero so that $\lambda_{ii}^{ph} = 0$ so as, following Mazin [30], the Coulomb pseudopotential matrix: $\mu_{ii}^*(\omega_c) = \mu_{ij}^*(\omega_c) = 0$ [30, 33, 37, 38]. As we discussed before the maximum value of the total electron-phonon coupling is estimated to be under 0.35 more or less similar to contribution, with opposite sign of Coulomb pseudopotential, so *in the first approximation,* and for reducing the number of free parameters, we put the two contributions equal to zero because they cancel each other out. Of course this doesn't means that the phonons are absent but just that the final result in the calculus of a lot of physical properties is not influenced by the their presence. Within these approximations, the electron-boson coupling-constant matrix λ_{ij} becomes: [30, 33, 37, 38]:

$$\lambda_{ij} = \begin{pmatrix} 0 & \lambda_{12}^{sf} & \lambda_{13}^{sf} \\ 0 & \lambda_{21}^{sf} = \lambda_{12}^{sf}\nu_{12} & 0 \\ \lambda_{31}^{sf} = \lambda_{13}^{sf}\nu_{13} & 0 & 0 \end{pmatrix} \tag{3}$$

where $\nu_{ij} = N_i(0)/N_j(0)$, and $N_i(0)$ is the normal density of states at the Fermi level for the i-th band. The coupling constants λ_{ij}^{sf} are defined through the electron-antiferromagnetic spin fluctuation spectral functions (Eliashberg functions) $\alpha_{ij}^2 F_{ij}^{sf}(\Omega)$. Following refs. [33, 37, 38] we choose these functions to have a Lorentzian shape, i.e.:

$$\alpha_{ij}^2 F_{ij}^{sf}(\Omega) = C_{ij}\{L(\Omega + \Omega_{ij}, Y_{ij}) - L(\Omega - \Omega_{ij}, Y_{ij})\}, \tag{4}$$

where

$$L(\Omega \pm \Omega_{ij}, Y_{ij}) = \frac{1}{(\Omega \pm \Omega_{ij})^2 + Y_{ij}^2}$$

and C_{ij} are normalization constants, necessary to obtain the proper values of λ_{ij}, while Ω_{ij} and Y_{ij} are the peak energies and the half-widths of the Lorentzian functions, respectively [38]. In all the calculations we set $\Omega_{ij} = \Omega_0$, i.e. we assume that the characteristic energy of spin fluctuations is a single quantity for all the coupling channels, and $Y_{ij} = \Omega_0/2$, based on the results of inelastic neutron scattering measurements [40].

The peak energy of the Eliashberg functions, Ω_0, can be directly associated to the experimental critical temperature, T_c, by using the empirical law $\Omega_0 = 2T_c/5$ that has

*THz electrodynamics of $BaFe_{1.91}Ni_{0.09}As_2$ film analyzed in the framework of multiband Eliashberg theory*6

been demonstrated to hold, at least approximately, for iron pnictides [41]. With all these approximations, necessary to reduce the number of free parameters, this is a more simple model that can still grasp the essential physics of iron compounds. We use a cut-off energy $\omega_c = 180$ meV and a maximum quasiparticle energy $\omega_{max} = 200$ meV.

The factors ν_{ij} that enter the definition of λ_{ij} (eq. 3) are unknown so we assume that they are equal to the Co doped [38] case so $\nu_{12} = 1.12$ and $\nu_{13} = 1$. In the same way we assume that also the coupling constant are similar to Co doped case [29] and we change lightly just a value for obtaining the correct critical temperature: $\lambda_{12} = 0.910$, $\lambda_{13} = 1.356$ and $\lambda_{23} = \lambda_{ii} = 0$ for a total coupling constant $\lambda_t = 2.17$.

We have calculated before, by solving Eliashberg equations on the imaginary axis for all temperatures under T_c, the temperature dependence of $\Delta_i(i\omega_{n=0})$ as is shown in Fig. 4 (dashed line) and then, using Padé approximants, we calculate the values of the gaps $\Delta_i(T)$ just at low temperatures. At the end we solve the Eliashberg equations on the real axis (solid line) and we calculate the values of $\Delta_i(T)$ in all temperature range under T_c. Of course the values calculated by Padé approximants [42] and by real axis solution are the same. The difference between $\Delta_i(i\omega_{n=0})$ and $\Delta_i(T)$ born from the fact that, in the weak coupling regime (BCS limit: electron-boson coupling constant less than one), the imaginary part of the complex functions $\Delta_i(\omega, T)$ and $Z_i(\omega, T)$ can be neglected so the values are almost the same while in the strong coupling regime this is not possible [43]. The gap values at low temperatures are $\Delta_1 = 4.3$ meV, $\Delta_2 = -2.8$ meV and $\Delta_3 = -5.9$ meV.

5. Calculation of the penetration depth

The penetration depth (or the superfluid density, see Fig. 5) can be computed starting from the gaps $\Delta_i(i\omega_n)$ and the renormalization functions $Z_i(i\omega_n)$ by

$$\lambda^{-2}(T) = (\frac{\omega_p}{c})^2 \sum_{i=1}^{3} w_i \pi T \sum_{n=-\infty}^{+\infty} \frac{\Delta_i^2(\omega_n) Z_i^2(\omega_n)}{[\omega_n^2 Z_i^2(\omega_n) + \Delta_i^2(\omega_n) Z_i^2(\omega_n)]^{3/2}} \tag{5}$$

where $w_i = (\omega_{p,i}/\omega_p)^2$ are the weights of the single bands, $\omega_{p,i}$ is the plasma frequency of the i-th band and ω_p is the total plasma frequency. Here, we can only act on the weights w_i^λ in order to adapt the calculation to the experimental $\lambda_L(T)$ [44]. The multiplicative factor that involves the plasma frequencies derives from the fact that the low-temperature value of the penetration depth $\lambda_L(0)$ should, in principle, be related to the plasma frequency by $\omega_p = c/\lambda_L(0)$. This is strictly valid only for a clean uniform superconductor at $T = 0$ if strong-coupling effects (or, more generally, Fermi-liquid effects) are negligible. In our case $w_1 = 0.05$, $w_2 = 0.80$ and $w_3 = 0.15$. We find from the fit that $\lambda(0) = 0.414$ μm.

*THz electrodynamics of $BaFe_{1.91}Ni_{0.09}As_2$ film analyzed in the framework of multiband Eliashberg theory*7

6. Discussion

The three-band Eliashberg model adequately describes experimental temperature dependences of the superfluid density and penetration depth of the $BaFe_{1.91}Ni_{0.09}As_2$ film. The calculated values of the larger gaps fall within the range reported in [6, 7, 8, 9, 10], the smaller gap correlates well with that found in [10]. The London penetration depth found in [5] for a $BaFe_{1.9}Ni_{0.1}As_2$ film was somewhat smaller ($\lambda_L \sim 226 \pm 20$ nm) compared to the present study, which can be ascribed to the different composition of our film. We can check the free input parameters values if we try to reproduce also the upper critical field B_{c2} in relation to temperature. In literature there are experimental data [45] relative to a bulk single crystal sample with a critical temperature between 18.8 K and 19.4 K and therefore very close to that of our film. There are also experimental data relative to epitaxial thin films [13] with $T_c = 17.2$ K. From the particular shape of the experimental curve that represents the temperature dependence of the upper critical field it can be understood that the system must be multiband [37]. The multiband Eliashberg model developed above can also be used to explain the experimental results of upper critical field measurements [37, 46, 47] as a function of temperature. For the sake of completeness, we give here the linearized gap equations in the presence of a magnetic field, for a superconductor in the clean limit (negligible impurity scattering). In the following, v_{Fj} is the Fermi velocity of band j, and H_{c2} is the upper critical field:

$$\omega_n Z_i(i\omega_n) = \omega_n + \pi T \sum_{m,j} \Lambda_{ij}(i\omega_n - i\omega_m)\text{sign}(\omega_m)$$

$$Z_i(i\omega_n)\Delta_i(i\omega_n) = \pi T \sum_{m,j}[\Lambda_{ij}(i\omega_n - i\omega_m) - \mu_{ij}^*(\omega_c)] \cdot$$
$$\cdot \theta(|\omega_c| - \omega_m)\chi_j(i\omega_m)Z_j(i\omega_m)\Delta_j(i\omega_m)$$

$$\chi_j(i\omega_m) = (2/\sqrt{\beta_j})\int_0^{+\infty} dq \exp(-q^2) \cdot$$
$$\cdot \tan^{-1}[\frac{q\sqrt{\beta_j}}{|\omega_m Z_j(i\omega_m)| + i\mu_B H_{c2}\text{sign}(\omega_m)}]$$

with $\beta_j = \pi H_{c2}v_{Fj}^2/(2\Phi_0)$. In these equations the three bare Fermi velocities v_{Fj} are the input parameters. The number of adjustable parameters can be reduced [37] to one by assuming that, as in a free-electron gas, $v_{Fj} \propto N_N^j(0)$ so that $v_{F2} = \nu_{21}v_{F1}$ and $v_{F3} = \nu_{31}v_{F1}$. We find $v_{F1} = 2.228 \times 10^5$ m/s for single crystal and 1.963×10^5 m/s for epitaxial thin films. In Fig. 6 the results of the theoretical calculations are shown and we can see that, in both cases, the agreement with the experimental data is good.

7. Conclusions

Using THz spectroscopy, we measured the far-infrared optical conductivity of $BaFe_{1.91}Ni_{0.09}As_2$ film in the normal and SC states. We found a clear signature of

*THz electrodynamics of BaFe$_{1.91}$Ni$_{0.09}$As$_2$ film analyzed in the framework of multiband Eliashberg theory*8

the SC gap, but the conductivity does not vanish in the SC state. The three-band Eliashberg approach was applied to describe this feature as well as the temperature dependences of the superfluid density and London penetration depth. Different independent experimental data (upper critical magnetic field versus temperature) seems confirm the choice of input parameters in the Eliashberg equations. Our results provide a strong evidence that BaFe$_{1.91}$Ni$_{0.09}$As$_2$ is a multi-band superconductor with $s_{\pm}$ pairing mediated by antiferromagnetic spin fluctuations.
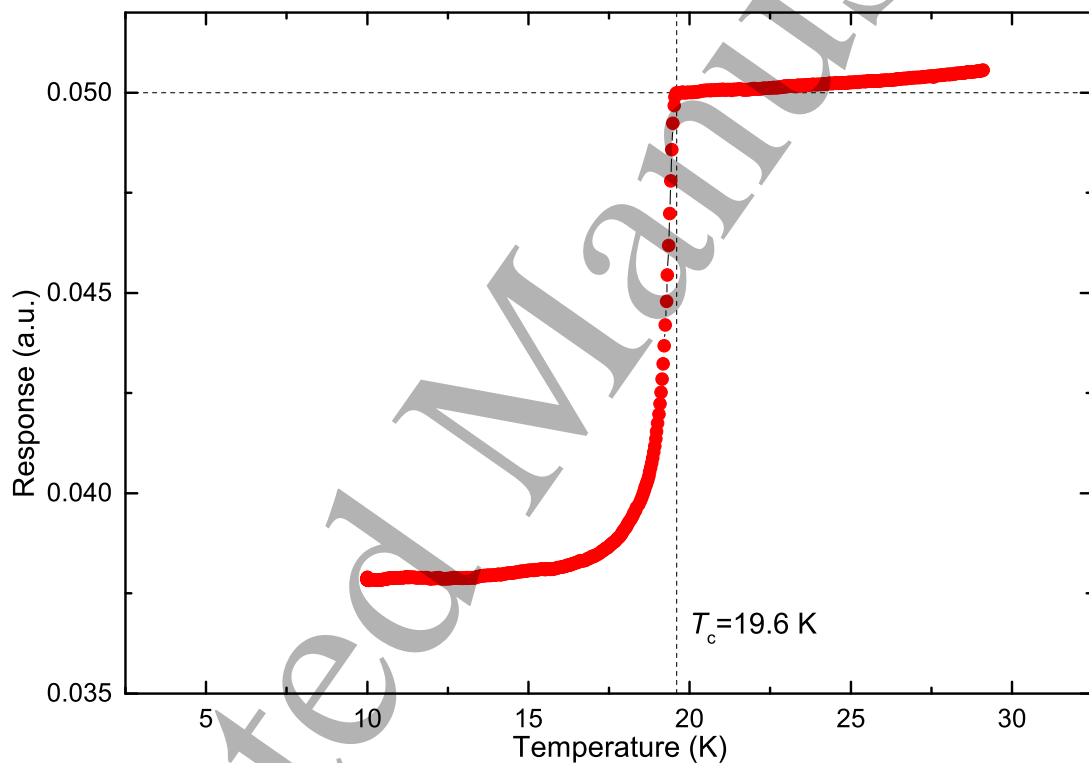
8. ACKNOWLEDGMENTS

[1] A.V. Chubukov, D.V. Efremov, and I. Eremin, *Phys.Rev. B* **78**, 134512 (2008).

[2] I.I. Mazin, D.J. Singh, M.D. Johannes, and M.H. Du, *Phys. Rev. Lett.* **101**, 057003 (2008).

[3] V. Grinenko, P. Materne, R. Sarkar, H. Luetkens, K. Kihou, C.H. Lee, S. Akhmadaliev, D.V. Efremov, S.-L. Drechsler, and H.-H. Klauss, *Phys. Rev. B* **95**, 214511 (2017).

[4] G. Ghigo, D. Torsello, G.A. Ummarino, L. Gozzelino, M.A. Tanatar, R. Prozorov, and P.C. Canfield, *Phys.Rev. Lett* **121**, 107001 (2018); Daniele Torsello, Roberto Gerbaldo, Laura Gozzelino, Makariy A. Tanatar, Ruslan Prozorov, Paul C. Canfield, Gianluca Ghigo, *Eur. Phys. J. Special Topics* **226**, 719–723 (2019).

[5] Sejun Yoon, Yu-Seong Seo, Seokbae Lee, Jeremy D. Weiss, Jianyi Jiang, MyeongJun Oh, Jongmin Lee, Sehun Seo, Youn Jung Jo, Eric E. Hellstrom, Jungseek Hwang, and Sanghan Lee, *Supercond. Sci. Technol.* **30**, 035001 (2017).

[6] Songxue Chi, Astrid Schneidewind, Jun Zhao, Leland W. Harriger, Linjun Li, Yongkang Luo, Guanghan Cao, Zhu'an Xu, Micheal Loewenhaupt, Jiangping Hu, and Pengcheng Dai, *Phys. Rev. Lett.* **102**, 107006 (2009).

[7] L. Ding, J.K. Dong, S.Y. Zhou, T.Y. Guan, X. Qiu, C Zhang, L.J. Li, X.Lin, G.H. Cao, Z.A. Xu, and S.Y. Li, *New J. Phys.* **11**, 093018 (2009).

[8] Y. Gong, W. Lai, T. Nosach, L.J. Li, G.H. Cao, Z.A. Xu, and Y.H. Ren, *New J. Phys.* **12**, 123003 (2010).

[9] Martin Dressel, Dan Wu, Neven Barišić, and Boris Gorshunov, *Journal of Physics and Chemistry of Solids* **72**, pp. 514–518 (2011).

[10] T.E. Kuzmicheva, V.A. Vlasenko, S.Yu. Gavrilkin, S.A. Kuzmichev, K.S. Pervakov, I.V. Roshchina, and V.M. Pudalov, *J. Supercond. Nov. Magn.* **29**, pp. 3059-3064 (2016).

[11] Paolo Dore, Boby Joseph, Stefano Lupi, Andrea Perucchi, *Novel Superconducting Materials* **1**, pp. 1–6 (2013).

[12] Stefan Richter, Saicharan Aswartham, Aurimas Pukenas, Vadim Grinenko, Sabine Wurmehl, Werner Skrotzki, Bernd Büchner, Kornelius Nielsch, and Ruben Hühne, *IEEE Transactions on Applied Superconductivity* **27**, 7300304 (2017).

[13] Stefan Richter, Fritz Kurth, Kazumasa Iida, Kirill Pervakov, Aurimas Pukenas, Chiara Tarantini,

THz electrodynamics of $BaFe_{1.91}Ni_{0.09}As_2$ film analyzed in the framework of multiband Eliashberg theory 9

Jan Jaroszynski, Jens Hänisch, Vadim Grinenko, Werner Skrotzki, Kornelius Nielsch, and Ruben Hühne, *Appl. Phys. Lett.* **110**, 022601 (2017).

[14] I. Shipulin, S. Richter, A. Anna Thomas, M. Brandt, S. Aswartham, R. Hühne, *Mater. Res. Express* **5**, 126001 (2018).

[15] S.Yu. Gavrilkin, O.M. Ivanenko, K.V. Mitsen, and A.Yu. Tsvetkov, *Bull. Lebedev Phys. Inst.* **41**, pp. 47–52 (2014).

[16] U.S. Pracht, E. Heitze, C. Clauss, D. Hafner, R. Bek, D. Werner, S. Gelhorn, M. Scheffler, M. Dressel, D. Sherman, B. Gorshunov, K.S. Il'in, D. Henrich, and M. Siegel, *IEEE Trans. THz Sci. Technol.* **3**, 269–280 (2013).

[17] R.P.S.M. Lobo, Y.M. Dai, U. Nagel, T. Rõõm, J.P. Carbotte, T. Timusk, A. Forget, D. Colson, *Phys. Rev. B* **82**, 100506 (2010).

[18] A.V. Chubukov, M.G. Vavilov, and A.B. Vorontsov, *Phys. Rev. B* **80**, 140515 (2009).

[19] V. Mishra, G. Boyd, S. Graser, T. Maier, P.J. Hirschfeld, and D.J. Scalapino, *Phys. Rev. B* **79**, 094512 (2009).

[20] J.P. Carbotte and E. Schachinger, *Phys. Rev. B* **81**, 104510 (2010).

[21] B. Muschler, W. Prestel, R. Hackl, T.P. Devereaux, J.G. Analytis, J.H. Chu, and I.R. Fisher, *Phys. Rev. B* **80**, 180510 (2009).

[22] H. Shiba, *Prog. Theor. Phys.* **40**, 435–451 (1968); **50**, 50–73 (1973).

[23] A.I. Rusinov, *JETP Lett.* **9**, 85–87 (1969); *Sov. Phys. JETP* **29**, 1101–1106 (1969).

[24] E. Schachinger and J.P. Carbotte, *Phys. Rev. B* **29**, 165–171 (1984).

[25] A.B. Vorontsov, M.G. Vavilov, and A.V. Chubukov, *Phys. Rev. B* **79**, 140507 (2009).

[26] E.J. Nicol and J.P. Carbotte, *Phys. Rev. B* **45**, 10519 (1992).

[27] D.N. Basov and T. Timusk, *Rev. Mod. Phys.* **77**, 721 (2005).

[28] T. Fischer, A.V. Pronin, J. Wosnitza, K. Iida, F. Kurth, S. Haindl, L. Schultz, B. Holzapfel, E. Schachinger, *Phys. Rev. B* **82**, 224507 (2010).

[29] D. Torsello, G.A. Ummarino, L. Gozzelino, T. Tamegai, and G. Ghigo, *Phys. Rev. B* **99**, 134518, (2019).

[30] P.J. Hirschfeld, M.M. Korshunov and I.I. Mazin, *Rep. Prog. Phys.* **74**, 124508 (2011); I.I. Mazin and J. Schmalian, *Physica C* **469**, 614–627 (2009).

[31] M. Tortello, D. Daghero, G.A. Ummarino, V. A. Stepanov, J. Jiang, J. D. Weiss, E.E. Hellstrom, and R.S. Gonnelli1, *Phys. Rev. Lett* **105**, 237002 (2010).

[32] Yuriy Yerin, Alexander Omelyanchouk, Stefan-Ludwig Drechsler, Dimitri V. Efremov, and Jeroen van den Brink, *Phys. Rev. B* **96**, 144513 (2017).

[33] G.A. Ummarino, M. Tortello, D. Daghero, R.S. Gonnelli, *Phys. Rev. B* **80**, 172503 (2009).

[34] G.M. Éliashberg, *Sov. Phys. JETP* **11**, 696–702 (1960).

[35] A.V. Chubukov, D. Pines, and J. Schmalian, *A Spin Fluctuation Model for d-Wave Superconductivity*; D. Manske, I. Eremin, and K.H. Bennemann, *Electronic Theory for Superconductivity in high-T_c Cuprates and Sr_2RuO_4*, K.H. Bennemann and J.B. Ketterson Editors, Volume II. Superconductivity: Novel Superconductors, Springer-Verlag Berlin Heidelberg (2008).

[36] D. Torsello, K. Cho, K.R. Joshi, S. Ghimire, G.A. Ummarino, N.M. Nusran, M.A. Tanatar, W.R. Meier, M. Xu, S.L. Bud'ko, P.C. Canfield, G. Ghigo, and R. Prozorov, *Phys. Rev. B* **100**, 094513 (2019).

[37] G.A. Ummarino, M. Tortello, D. Daghero, R.S. Gonnelli, *J. Supercond. Nov. Magn.* **24**, 247–253 (2011).

[38] G.A. Ummarino, *Phys. Rev. B* **83**, 092508 (2011).

[39] L. Boeri, M. Calandra, I.I. Mazin, O.V. Dolgov, F. Mauri, *Phys. Rev. B* **82**, 020506 (2010).

[40] D.S. Inosov, J.T. Park, P. Bourges, D.L. Sun, Y. Sidis, A. Schneidewind, K. Hradil, D. Haug, C.T. Lin, B. Keimer and V. Hinkov, *Nature Physics* **6**, 178–181 (2010).

[41] D.S. Inosov, J.T. Park, A. Charnukha, Yuan Li, A.V. Boris, B. Keimer, and V. Hinkov, *Phys. Rev. B* **83**, 214520 (2011).; J. Paglione and R.L. Greene, *Nature Physics* **6**, 645–658 (2010).

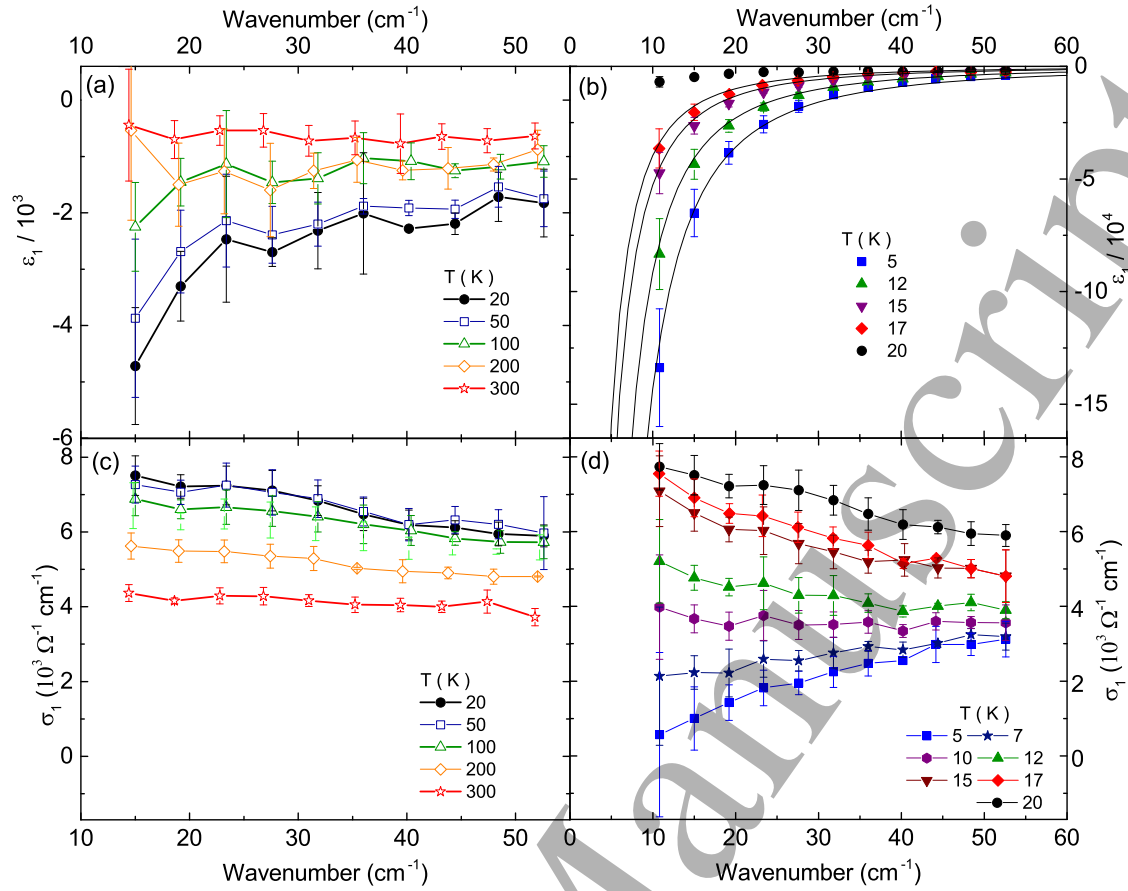[42] G.A. Ummarino, Eliashbeg theory, Emergent Phenomena in Correlated Matter edited by Eva

THz electrodynamics of $BaFe_{1.91}Ni_{0.09}As_2$ film analyzed in the framework of multiband Eliashberg theory10

Pavarini, Erik Koch and Ulrich Schollwock, published by Forschungszentrum Julich Gmbh and Institute for Advanced Simulations, 23-27 September 2013 Volume 3, Pages 13.1-13.36, ISSN 2192-8525 ISBN 978-3-89336-884-6.

[43] A.E. Karakozov, E.G. Maksimov, A.A. Mikhailovsky, *Solid State Communications*, **79**, 329–335 (1991); F. Marsiglio, J.P. Carbotte *Phys. Rev. B* **43**, 5355 (1991); J.P. Carbotte, F Marsiglio B. Mitrovich, *Phys. Rev. B* **33**, 6135 (1986).

[44] G. Ghigo, G. A. Ummarino, L. Gozzelino, R. Gerbaldo, F. Laviano, D. Torsello, T. Tamegai, *Scientific Reports* **7**, 13029 (2017).

[45] N. Ni, A. Thaler, J.Q. Yan, A. Kracher, E. Colombier, S.L. Budko, P.C. Canfield, and S.T. Hannahs, *Phys. Rev. B* **82**, 024519 (2010).

[46] H. Suderow, V.G. Tissen, J.P. Brison, J.L. Martínez, S. Vieira, P. Lejay, S. Lee, and S. Tajima, *Phys. Rev. B* **70**, 134518 (2004).

[47] Y. Yerin, S.-L. Drechsler, G. Fuchs, *Journal of Low Temperature Physics* **173** (5-6), 247–263 (2013).
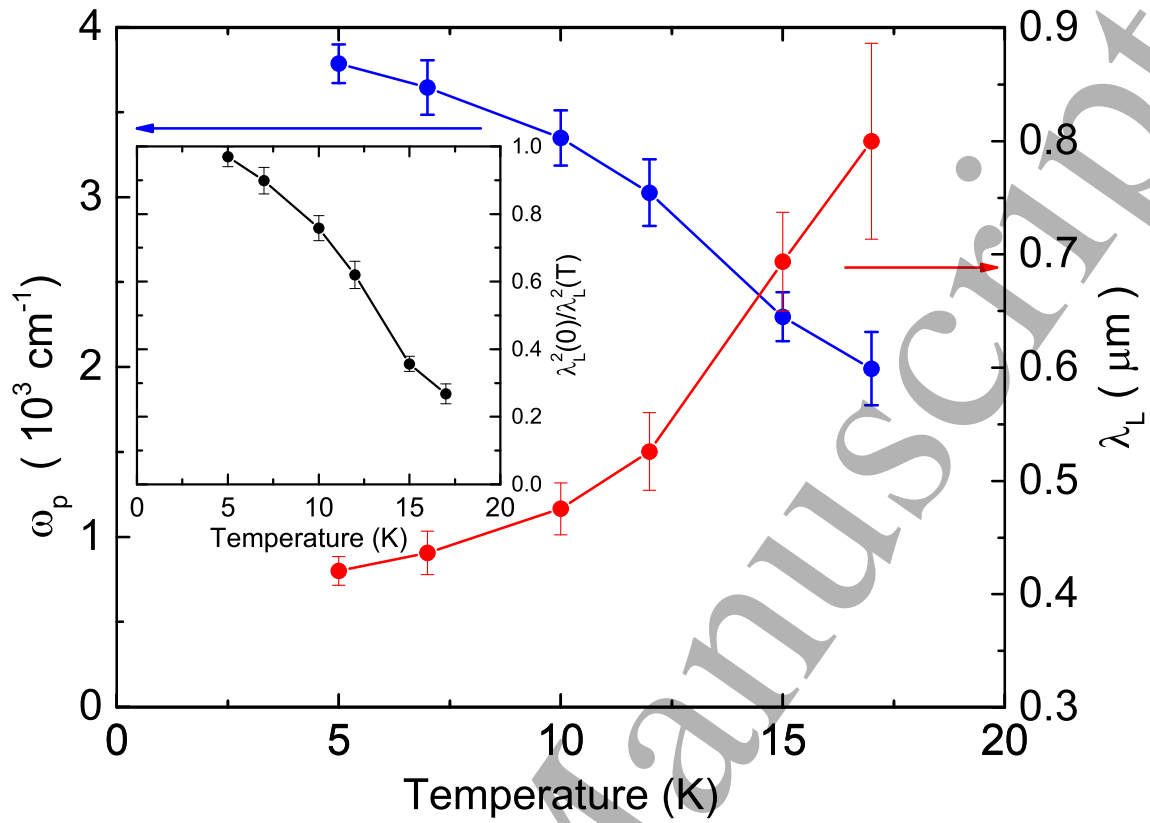

Figure 1. (Color online) The temperature of SC transition T_c of Ni-Ba122 film determined by the change in the magnetic susceptibility of the sample in inductive technique.

THz electrodynamics of $BaFe_{1.91}Ni_{0.09}As_2$ film analyzed in the framework of multiband Eliashberg theory 1
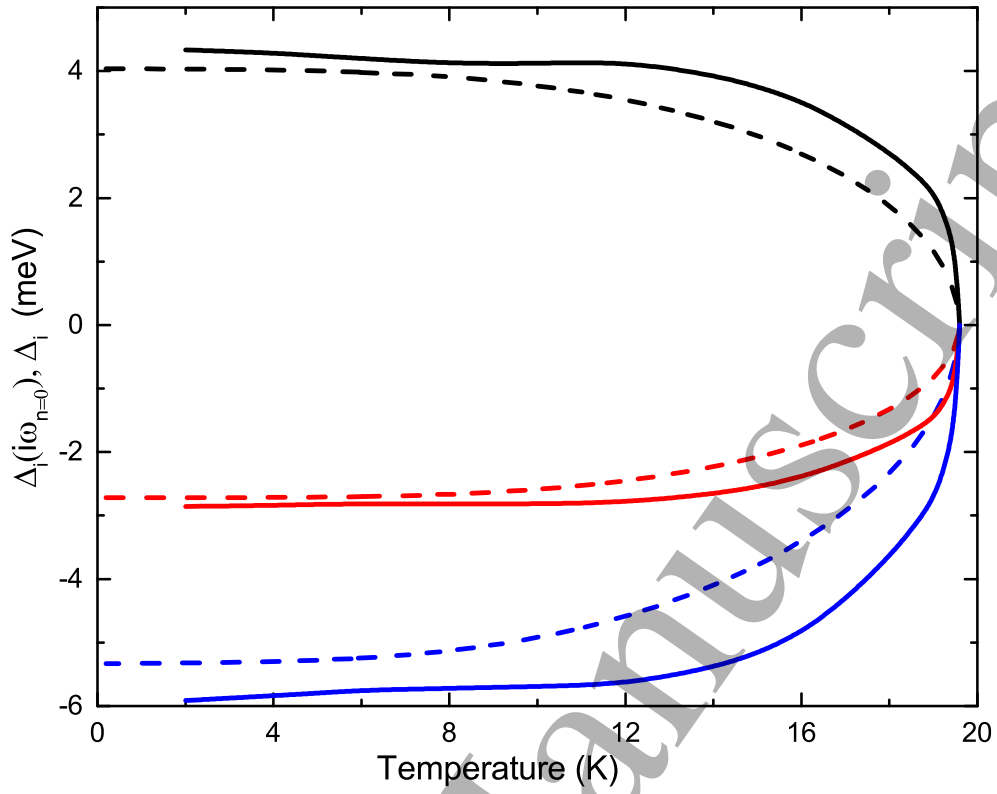

Figure 2. (Color online) Spectra of the permittivity ε_1 and the conductivity σ_1 in the normal (a,c) and SC (b,d) phases. Solid lines in (b) show a fit of the spectra by the relation $\varepsilon_1 \propto -(\omega_{p,s}/\omega)^2$.

THz electrodynamics of $BaFe_{1.91}Ni_{0.09}As_2$ film analyzed in the framework of multiband Eliashberg theory12
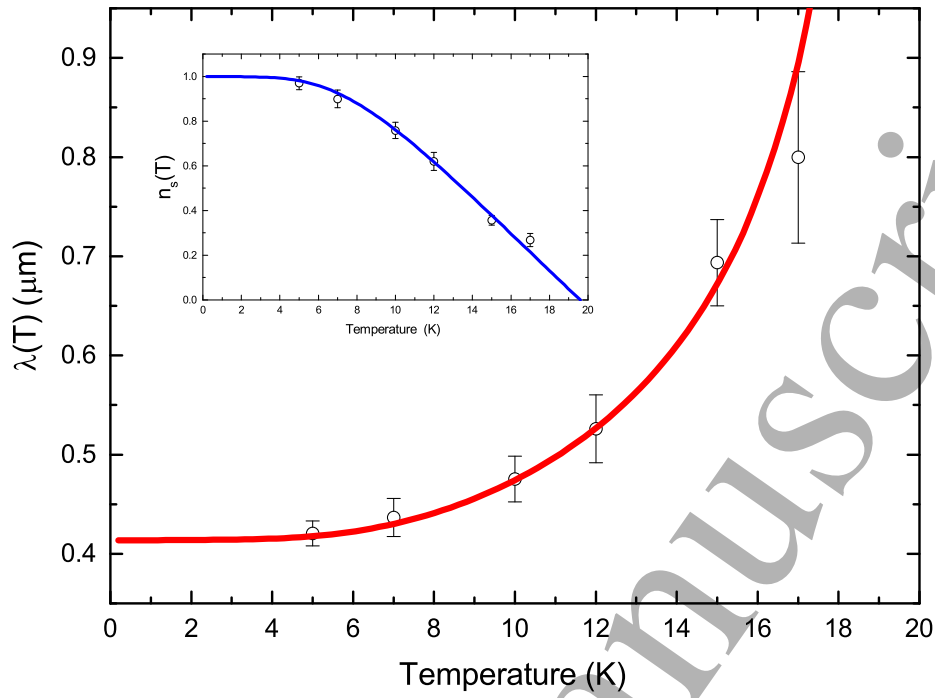

Figure 3. (Color online) Temperature dependences of the plasma frequency of the SC condensate (left scale) and of the London penetration depth (right scale). The temperature dependence of superfluid density $n_s = [\lambda_L(0)/\lambda_L(T)]^2$ is shown in the inset.

*THz electrodynamics of $BaFe_{1.91}Ni_{0.09}As_2$ film analyzed in the framework of multiband Eliashberg theory*1

Figure 4. (Color online) The gaps $\Delta_i(i\omega_{n=0})$ as a function of temperature obtained by solving the Eliashberg equations on imaginary axis (dashed lines: black band 1, red band 2 and dark blue band 3) and real axis (solid lines).
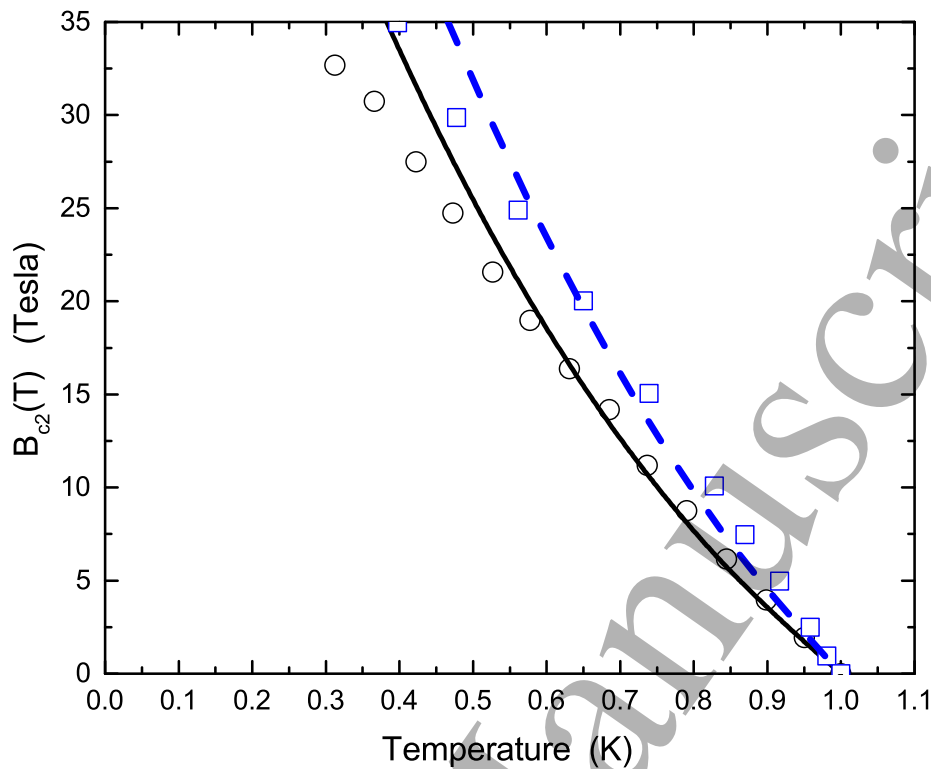
*THz electrodynamics of $BaFe_{1.91}Ni_{0.09}As_2$ film analyzed in the framework of multiband Eliashberg theory*14

Figure 5. (Color online) The experimental penetration depth against the temperature and the theoretical curve obtained by solving the Eliashberg equations. In the inset the experimental superfluid density as a function of temperature is shown and the theoretical curve obtained by solving the Eliahsberg equations.

*THz electrodynamics of $BaFe_{1.91}Ni_{0.09}As_2$ film analyzed in the framework of multiband Eliashberg theory*1(

Figure 6. (Color online) The experimental upper critical field parallel to c axis versus temperature from [45] (black open circles) and from [13] (blue open squares). The theoretical curves obtained by solving the Eliahsberg equations are shown by black solid line and blue dashed line. The experimental data are normalized to onset critical temperature of 18.8 K and 17.6 K.